Position Control of Brushless DC Motor Using Improved Ant Colony Optimization Based Fuzzy PD Controller

Xingyan Mou

School of Electrical Engineering
and Automation,Wuhan University, Wuhan 430000, China
2021302191190@whu.edu.cn

Abstract. Accurate brushless DC motor position control is the basis for realizing various high-precision control systems. In order to achieve precise control of brushless DC motor position and improve control stability, this paper proposes a fuzzy PD control method based on the improved ant colony optimization (ACO). On the basis of the mathematical model of BLDC motor, an improved ant colony optimization (IACO)is proposed, maximizing the dynamic balance between the global search capability and convergence speed of ACO. A fuzzy PD controller based on IACO is designed, where IACO is used for real-time optimization and the tuning of the fuzzy PD controller parameters, which significantly reduces the difficulty and accuracy of parameterization. The BLDC closed-loop position control simulation model is built in Simulink, and the simulation is carried out using traditional PD, ACO PD, fuzzy PD, IACO fuzzy PID, and the comparison experiments are conducted under the step signal, perturbation signal, and following signal, respectively. The simulation results show that BLDC position control based on the IACO optimized fuzzy PD controller can significantly increases the response speed and reduce the overshoot and has a strong anti-interference ability, which effectively improves the control accuracy, dynamic performance and robustness of the system.

Keywords: Brushless dc motor, Fuzzy PD control, Position control, Ant colony optimization

1 Introduction

Brushless DC motor (BLDC) is widely used in aerospace, home appliance, automotive and other industrial fields for its excellent speed regulation characteristics, high electromechanical conversion ratio and other advantages [1]. With the development of technology, realizing high accuracy and high robustness of position control is the key to automation systems such as robotic arms, CNC machine tools, etc. [2], and the design of a high-precision position control method for brushless DC motors is essential to improve the performance of the whole system.

In terms of precise motor position control, the PD control strategy has been widely adopted due to its simplicity and efficiency. The PD controller achieves fast and

Y. Yue (ed.), *Proceedings of the 2024 International Conference on Mechanics, Electronics Engineering and Automation (ICMEEA 2024)*, Advances in Engineering Research 240,
https://doi.org/10.2991/978-94-6463-518-8_34

stable control effect by adjusting the P and D2 parameters. Researcher used a trajectory tracking control method based on self-coupled PD (SCPD) to achieve fast and stable tracking of the desired trajectory of a quadrotor UAV [3]; Researcher used a PD control algorithm based on the sliding mode function compensation to achieve high-precision gait control of a lower limb exoskeleton robot [4]. The PD control performs well in applications that require fast response and minimal overshoot.

Since the environment in real application scenarios is more complex and changeable and easily affected by uncertainties, the parameters of the traditional PD controller are difficult to ensure that the control effect is always in the optimal state [5], for this reason, fuzzy logic control is introduced into the PD control framework to form a fuzzy PD controller. Researcher used fuzzy PD control to compensate for the nonlinear motion characteristics of an intelligent lawn mower and realize accurate following of the planned motion direction [6]. The fuzzy PD controller combines the nonlinear characteristics of fuzzy logic and the simplicity of PD control, which can better deal with system uncertainties and parameter variations, and enhances the control system's adaptability and resilience.

Despite the improved control performance of fuzzy PD control, the parameter settings of the controller usually require extensive manual debugging and experience-based tuning. In this regard, intelligent optimization algorithms, such as ant colony optimizations, provide effective solutions for optimizing fuzzy controller parameters. In literature [7], IPSO was applied to the PID control of PSFB, which achieves better control accuracy and convergence speed; literature proposes an aspen [8].

The work proposed an improved fuzzy neural network PID algorithm with Beetle Swarm Optimization (BSO), which effectively improved the robustness and dynamic capability of the system [9].

Ant colony optimization (ACO) is an optimization method that mimics how ants forage in the wild and is particularly effective at resolving challenging optimization issues. Researcher optimized the cold chain logistics path based on hybrid ACO algorithm, which significantly improved the efficiency of the model [10].

By applying the ant colony optimization to automatically adjust the rules and parameters of the fuzzy PD controller, the performance of the system can be further enhanced, especially in dynamic environments. However, the ant colony optimization has to be improved because it converges slowly and is prone to finding local optimal solutions.

The aim of this study is to investigate the effectiveness of the fuzzy PD control optimized by the improved ant colony optimization in the position control of a brushless DC motor. The mathematical model of BLDC is established, and an improved ACO algorithm(IACO) is proposed and applied to the fuzzy PD controller. By comparing with the PD control, the fuzzy PD control, the PD control optimized by ACO and the fuzzy PD control optimized by IACO, the efficacy of the IACO optimized fuzzy PD controller is examined and confirmed in terms of improving the system's adaptability and control precision.

2 Mathematical Model of BLDC

When establishing the mathematical model of BLDC, this paper follows the following assumptions [11]: the internal structures of the motor are all ideal; the effects of magnetic circuit saturation, eddy current losses, hysteresis losses, armature reaction, and other factors are ignored; and the system uses devices with good switching characteristics.

The resulting BLDC stator voltage balance equation is shown below:

$$\begin{bmatrix} U_A \\ U_B \\ U_C \end{bmatrix} = \begin{bmatrix} R_A & 0 & 0 \\ 0 & R_B & 0 \\ 0 & 0 & R_C \end{bmatrix} \begin{bmatrix} i_A \\ i_B \\ i_C \end{bmatrix} + \frac{d}{dt} \begin{bmatrix} L_A & L_{AB} & L_{AC} \\ L_{BA} & L_B & L_{BC} \\ L_{CA} & L_{CB} & L_C \end{bmatrix} \begin{bmatrix} i_A \\ i_B \\ i_C \end{bmatrix} + \begin{bmatrix} e_A \\ e_B \\ e_C \end{bmatrix} \quad (1)$$

$U_A, U_B, U_c$are stator phase voltages;$R_A, R_B, R_C$are stator phase resistances;$i_A, i_B, i_C$are stator phase currents; $L_A, L_B, L_C, L_{AB}, L_{AC}, L_{BA}, L_{BC}, L_{CA}, L_{CB}$ are stator winding self-inductance and mutual inductance, respectively; e_A, e_B, e_C are stator counter electromotive forces.

Because of the stator phase resistance and winding self-inductance , mutual inductance satisfy the following conditions:

$$L_A = L_B = L_C = L \quad (2)$$

$$R_A = R_B = R_C = R \quad (3)$$

$$L_{AB} = L_{AC} = L_{BA} = L_{BC} = L_{CA} = L_{CB} = M \quad (4)$$

And equations (5) and (6) can be obtained from the BLDC structure:

$$i_A + i_B + i_C = 0 \quad (5)$$

$$Mi_A + Mi_B + Mi_C = 0 \quad (6)$$

$i_A, i_B, i_C$are the three−phase currents A, B, C respectively;$Mi_A, Mi_B, Mi_C$are the mutual inductance of the stator winding and the sum of the products of the currents in each phase respectively.

Combining equations (1) (2) (3) (4) (5) (6) leads to the following equation:

$$\begin{bmatrix} U_A \\ U_B \\ U_C \end{bmatrix} = \begin{bmatrix} R & 0 & 0 \\ 0 & R & 0 \\ 0 & 0 & R \end{bmatrix} \begin{bmatrix} i_A \\ i_B \\ i_C \end{bmatrix} + \begin{bmatrix} L-M & 0 & 0 \\ 0 & L-M & 0 \\ 0 & 0 & L-M \end{bmatrix} \frac{d}{dt} \begin{bmatrix} i_A \\ i_B \\ i_C \end{bmatrix} + \begin{bmatrix} e_A \\ e_B \\ e_C \end{bmatrix} \quad (7)$$

In this model, assuming that the currents in the AB-phase windings are in opposite directions and of the same amplitude, and ignoring the transient changes in commutation, the following equation can be obtained from (7):

$$U_{AB} = r_a i_d + L_a \frac{di_d}{dt} + C_e \Omega \quad (8)$$

$r_a$is the line resistance of the armature winding;$L_a$is the equivalent inductance;C_e is the coefficient of reverse electromotive force;$\Omega$is the mechanical angle.

The following equation can be obtained from the torque balance characteristic of the motor:

$$T_e - T_l = J \frac{d\Omega}{dt} \quad (9)$$

T_e is the electromagnetic torque; T_l is the load torque; J is the moment of inertia. Under rated excitation, the following equation is obtained:

$$T_e = C_m i_d \quad (10)$$

When the motor is unloaded, the armature current expression can be obtained from (9)(10):

$$i_d = \frac{J}{C_m}\frac{d\Omega}{dt} \tag{11}$$

The differential equation for the armature voltage U_d is obtained from (8)(11):

$$U_d = \frac{L_a J}{C_m}\frac{d^2\Omega}{dt} + \frac{r_a J}{C_m}\frac{d\Omega}{dt} + C_e\Omega \tag{12}$$

The motor's transfer function is obtained after Laplace transform:

$$U_d = \frac{L_a J}{C_m}\frac{d^2\Omega}{dt} + \frac{r_a J}{C_m}\frac{d\Omega}{dt} + C_e\Omega \tag{13}$$

The final transfer function of BLDC is obtained as follows, and the system structure is shown in the Fig. 1 below, which is a second-order system:

$$G(s) = \frac{1/C_e}{T_l T_m s^2 + T_m s + 1} \tag{14}$$

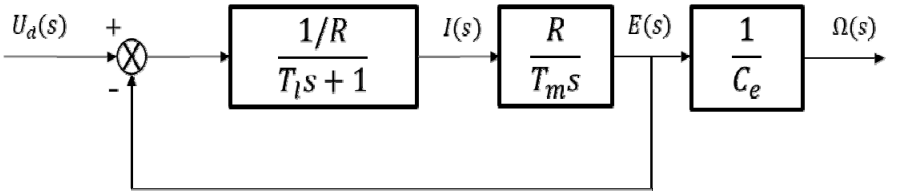

Fig. 1. Structure of the BLDC transfer function system (Photo credited: Original)

Where T_l and T_m are the electromagnetic and mechanical time constants of the motor, respectively, expressed as follows:

$$T_l = \frac{L_a}{r_a} = \frac{L}{R} \tag{15}$$

$$T_m = \frac{GD^2 r_a}{375 C_e C_m} = \frac{J r_a}{C_e C_m} = \frac{2JR}{C_e C_m} \tag{16}$$

In this paper, The BLDC transfer function used in the experiment is defined as follows:

$$G(s) = \frac{3}{0.1s^2 + s + 1} \tag{17}$$

3 Fuzzy PD Controller Design

The traditional PID controller consists of proportional (P), integral (I), and differential (D), which adjusts the control inputs according to the current error of the control system to realize precise control. In the closed-loop position control of BLDC, there is a very high demand for position accuracy, and the system response should be as fast as possible without overshoot [12]. Due to the differential loop's hysteresis and severe sensitivity to changes in the bias signal, it is necessary to avoid overshoot and provide a quick transient response, and avoid the potential steady state problem caused by the integral effect, this study removes the integral loop of the PID and adopts the PD control. The formula and structure of PD control are shown in equation (18) and Fig. 2 respectively, where K_p is the scaling factor, K_d is the differentiation factor and $e(t)$ is the tracking error.

$$u(t) = K_p e(t) + K_d \frac{de(t)}{dt} \quad (18)$$

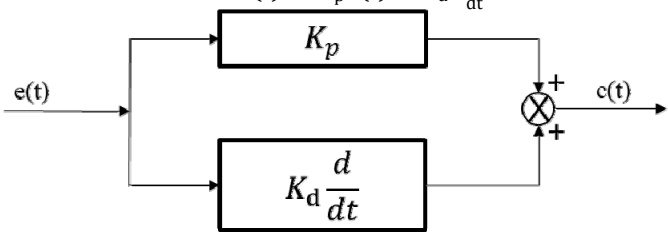

Fig. 2. Structure of the traditional PD controller (Photo credited: Original)

The traditional PD control can not be adjusted accordingly when the parameters and the system change, and the control performance can not meet the standard, the fuzzy PD controller overcomes the shortcomings of the PD that can not adjust the parameters in real time, especially suitable for dealing with the complex and changing control environment. The fuzzy PD controller inputs the system error E and the rate of change of the error E_c and then carries out the fuzzification process, and then it is handed over to the fuzzy controller for fuzzy inference, and then the defuzzification outputs the integrating proportionality coefficients U, and finally obtains the values of K_p and K_d, and the control equations are shown as follows:

$$u(t) = \left(K_e * e(t) + K_{ec} * \frac{de(t)}{dt}\right) * K_u \quad (19)$$

Where K_e is the error coefficient; K_{ec} is the error change rate coefficient; K_u is the rectification ratio coefficient, which determines the size of K_p and K_d.The relationship of each parameter is shown below:

$$K_p = K_u * K_e \quad (20)$$

$$K_d = K_u * K_{ec} \quad (21)$$

The fuzzy pd controller is constructed using fuzzy logic designer in MATLAB, the inference system is a mamdami fuzzy system, and the calculations for refining are performed using the center of gravity approach. The rule base for fuzzy PD controller and the relationship of K_u with inputs are shown in the Table 1 and Fig. 3 respectively, and the inputs are distributed with seven triangular membership functions, denote by Negative Big(NB), Negative Medium(NM), Negative Small(NS), Zero (O), Positive Small(PS), Positive Medium (PM), and Positive Big (PB), the fuzzy domains are all [-6, 6]. The distribution of the affiliation function of e is shown in the Fig. 4, and the affiliation functions of the other two variables are the same as theirs.

Table 1. Rule base for fuzzy PD controller

E \ E_c	NB	NM	NS	O	PS	PM	PB
NB	PB	PB	PB	PB	PM	O	O
NM	PB	PB	PB	PB	PM	O	O

NS	PM	PM	PM	PM	O	NS	NS
O	PM	PM	PS	O	NS	NM	NM
PS	PS	PS	O	NM	NM	NM	NM
PM	O	O	NM	NB	NB	NB	NB
PB	O	O	NM	NB	NB	NB	NB

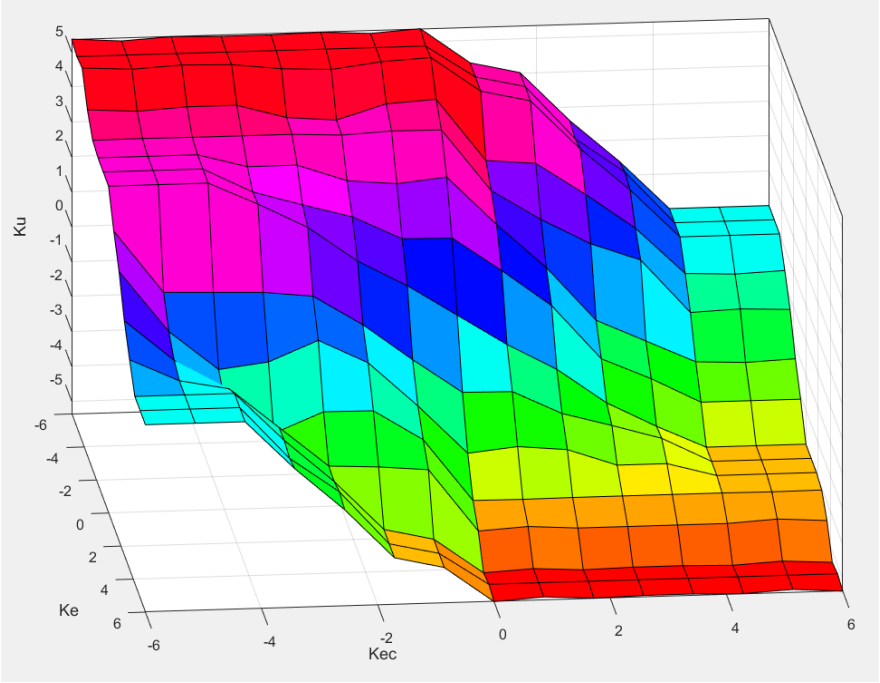

Fig. 3. Relationship of K_u with inputs (Photo credited: Original)

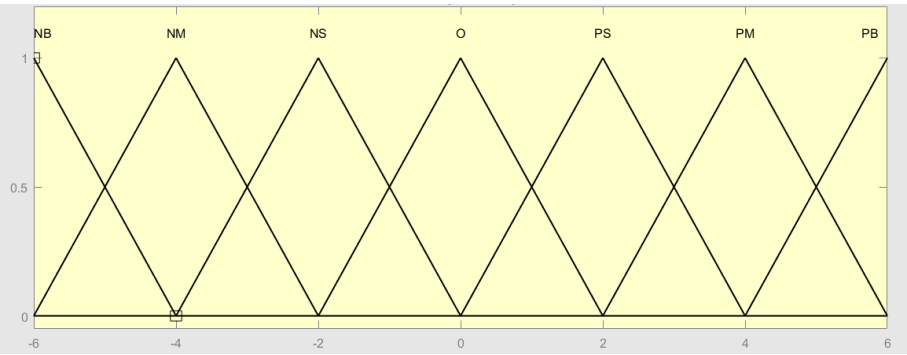

Fig. 4. The membership function of E (Photo credited: Original)

4 Improved Ant Colony Optimization

4.1 Ant Colony Optimization

Ant Colony Optimization (ACO) algorithm has strong global search capability and robustness, and is an efficient heuristic algorithm for parallel search [13].

In nature, ants release pheromones on their traveling paths while searching for food, the journey length and the pheromone concentration are negatively correlated, these pheromones will be detected by other ants, who will then follow the trail where the concentration of pheromones is greatest. Over time, the shortest path accumulates the most pheromone, which attracts more ants to take this path, forming a positive feedback and ultimately optimizing the route of the whole colony.

Let there be m ants that are randomly placed at n locations, and the probability p_{ij}^{k} that ant k will move from place i to place j at moment t is given by the following formula:

$$p_{ij}^{k} = \begin{cases} \dfrac{\tau_{ij}^{\alpha}(t)\eta_{ij}^{\beta}(t)}{\sum_{S\in allow_k}\tau_{is}^{\alpha}(t)\eta_{is}^{\beta}(t)}, & S \in allow_k \\ 0, & S \notin allow_k \end{cases} \tag{22}$$

Where τ_{ij} denotes the pheromone concentration on path ij at moment t;$\eta_{ij}(t) = \frac{1}{d_{ij}}$, d_{ij} denotes the distance between places i and j; α denotes the pheromone's importance;βdenotes the expected heuristic factor.

When all ants have completed one cycle, the pheromone is updated according to the following equation:

$$\tau_{ij}(t+n) = (1-\rho)\tau_{ij}(t) + \Delta\tau_{ij} \tag{23}$$

$$\Delta\tau_{ij} = \sum_{k=1}^{m} \Delta\tau_{ij}^{k} \tag{24}$$

ρ denotes the pheromone evaporation coefficient; $\Delta\tau_{ij}$ denotes the pheromone increment on trajectory ij in this iteration; $\Delta\tau_{ij}^{k}$ denotes the amount of pheromone that the kth ant has left on trajectory ij in this iteration, and the expression is as follows:

$$\Delta\tau_{ij}^{k}(t) = \begin{cases} \frac{Q}{L_k}, \text{If the Kth ant visits j from i in this loop} \\ 0, \qquad\qquad \text{otherwise} \end{cases} \tag{25}$$

L_k denotes the length of the path traveled by the kth ant in this cycle; Q denotes the total amount of pheromone released by an ant completing a path walk.α reflects the role of pheromone strength on the influence on the ants, α the larger, the ants will be more inclined to choose the path that other ants have traveled, the faster the speed of convergence; β reflects the strength of the role of the deterministic and a priori factors of the ant colony in the process of searching for paths, β the larger, the greater the possibility of ants to carry out the transfer, the faster the speed of convergence; ρ reflects the degree of mutual influence of individuals in the ant colony, the larger ρ is, the stronger the global search ability and search randomness of the algorithm is, and the slower the convergence speed is.

4.2 Improved Ant Colony Optimization

The lengthy search period and ease of stagnation and local optimal solution falloff are the drawbacks of ACO. In order to improve the global search ability of ACO and refrain from settling for locally best solutions, this paper improves the adaptive pheromone importance α, the expected heuristic factor β, and the pheromone evaporation coefficient ρ, in order to optimize the dynamic balance between the ACO's convergence speed and its capacity for global searches.

At the beginning of the search, pheromone cannot be used as the main search condition because the number of ants and pheromone are small, so it is important to focus on the evaluated performance index as the main parameter, and at the same time, increase the pheromone evaporation speed to improve the global search capability. When the search is about to end, the pheromone is used as the main search condition because the number of ants and pheromone are gradually increasing, and the evaluated performance index is used as the secondary search factor, while the pheromone evaporation coefficient is reduced to speed up the convergence progress. The expression of each parameter after improvement are as follows:

$$\alpha(k) = a^{\sqrt{\frac{k}{G}}} \cdot \text{rand} \tag{26}$$

$$\beta(k) = 1 - e^{b\left(1-\frac{k}{G}\right)} \cdot \text{rand} \tag{27}$$

α is the evaporation coefficient adaptive factor; β is the evaporation coefficient adaptive factor; G is the total number of iterations; k is the current number of iterations; rand is a random number between $(0,1)$.

$$\rho(k) = \frac{\varphi}{1+\gamma e^{\frac{k}{G}}} \tag{28}$$

φ is the constant term; $\gamma$is the evaporation coefficient adaptive factor.

5 Position Control of BLDC

5.1 System Structure

The structure of the fuzzy PD position control system for BLDC is shown in Fig. 5. The environment is built in MATLAB 2022b with Simulink for simulation experiments, and the simulation model is shown in Fig. 6, 7 and 8. The IACO parameters are shown in Table 2.

The three parameters of the fuzzy PD controller are optimized and calibrated by IACO to find the optimal values of the PD coefficients in the system to achieve the best positional control of the BLDC. After the simulation, IACO is used to adjust the parameters of the fuzzy PD controller to obtain the optimal PD control parameters that Kp=0.7953, Kd=0.7003.

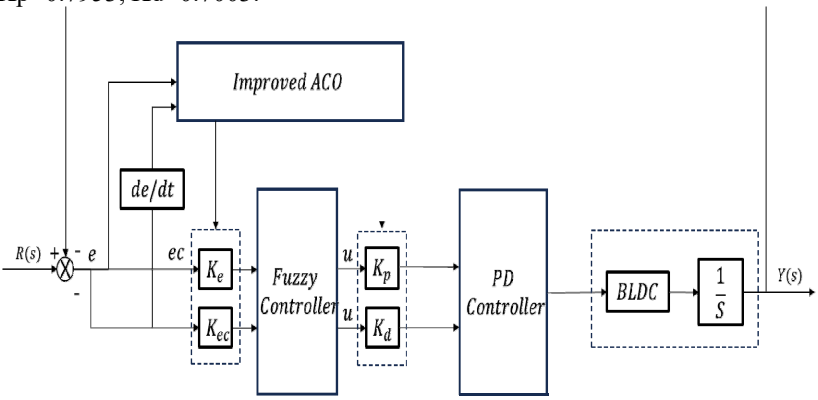

Fig. 5. Position control system of BLDC (Photo credited: Original)

Table 2. Parameter Settings of IACO

Parameter Settings			
a	0.6	m	50
b	0.8	n	1000
φ	1.15	G	100
γ	1		

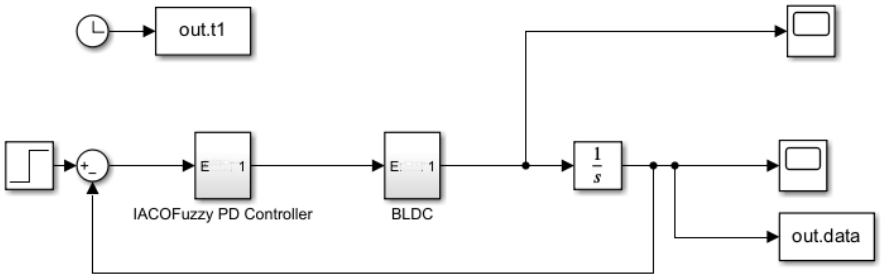

Fig. 6. System Simulation Model (Photo credited: Original)

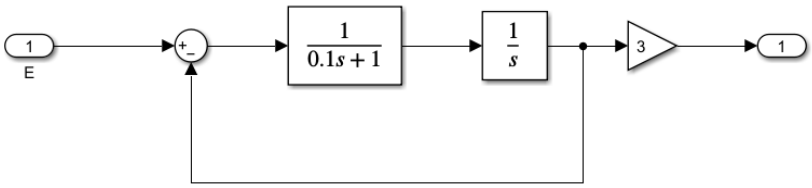

Fig. 7. Simulation model of BLDC (Photo credited: Original)

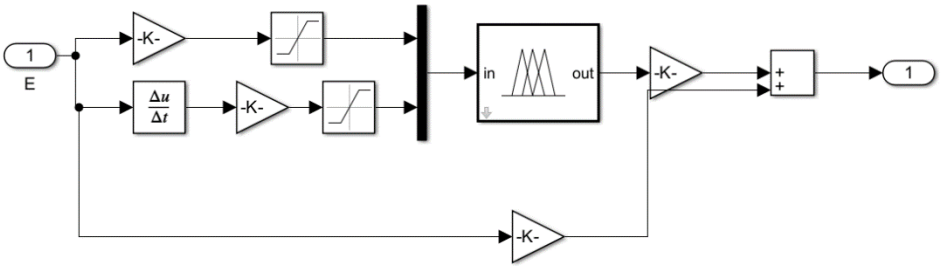

Fig. 8. Simulation model of fuzzy PD controller (Photo credited: Original)

The position control of BLDC is carried out using conventional PD, ACO-tuned PD, fuzzy PD and IACO fuzzy PD controllers for unit step experiments, perturbation experiments and signal following experiments respectively and compared. Among them, the parameters of the conventional PD are set using the Ziegler-Nichols method and empirical fine-tuning.

5.2 Step Signal

The response curve of the 4 systems at a unit step signal are shown in Fig. 9 and Fig. 10:

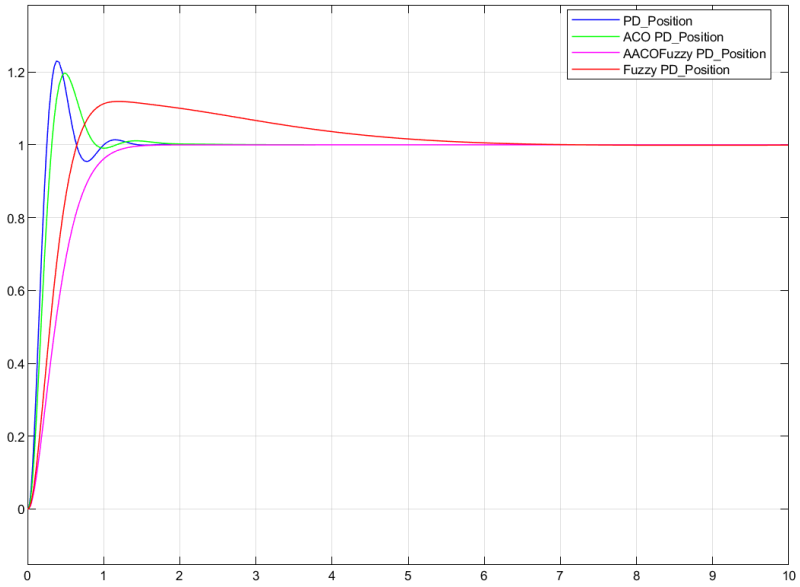

Fig. 9. Position response curve under unit step signal (Photo credited: Original)

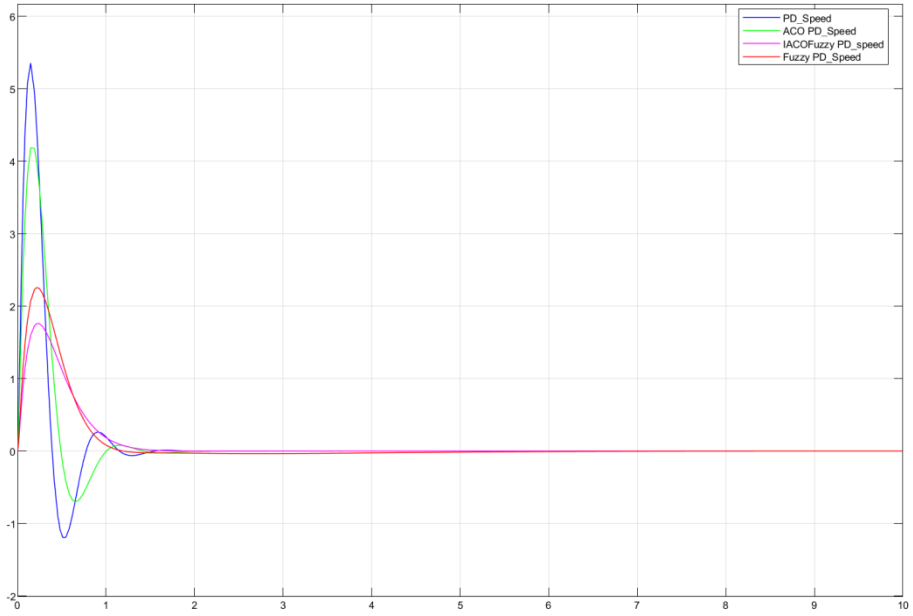

Fig. 10. Speed response curve under unit step signal (Photo credited: Original)

Table 3. Position control performance comparison under step signal

	Max Value	Settling time	Overshoot

PD	1.23	2.347	18.70%
ACO PD	1.197	3.062	16.46%
Fuzzy PD	1.119	6.57	10.63%
IACO Fuzzy PD	1	1.756	0

As can be seen from Fig. 9, relative to PD and ACO PD, Fuzzy PD reduces the amount of overshoot but greatly prolongs the settling time, while IACO Fuzzy PD not only further disappears the amount of overshoot completely on the basis of the original one, but also greatly shortens the settling time. As shown in the Table 3, IACO fuzzy PD reduced the settling time by 25.18%, 42.65%, and 73.27% over PD, ACO PD, and Fuzzy PD, respectively. Meanwhile, as can be seen from Fig. 10, the overshoot of speed is also small, which increases the stability of the system.

5.3 Disturbance Signal

Random white noise, with a noise power of 0.0003 and a sampling time of 0.05, which is shown in the Fig. 11, was added to the unit step signal. Comparisons are made in the interval after all signal steps have been stabilized.

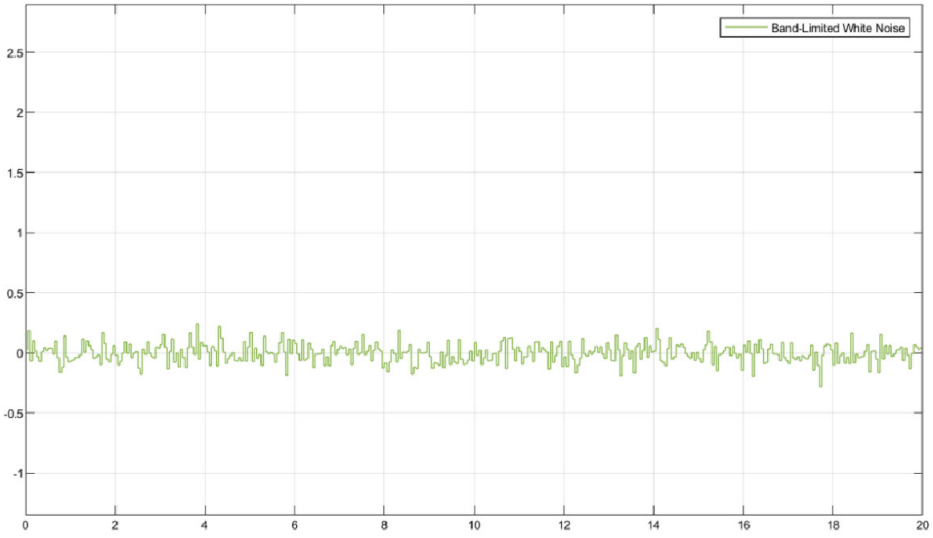

Fig. 11. White noise curve (Photo credited: Original)

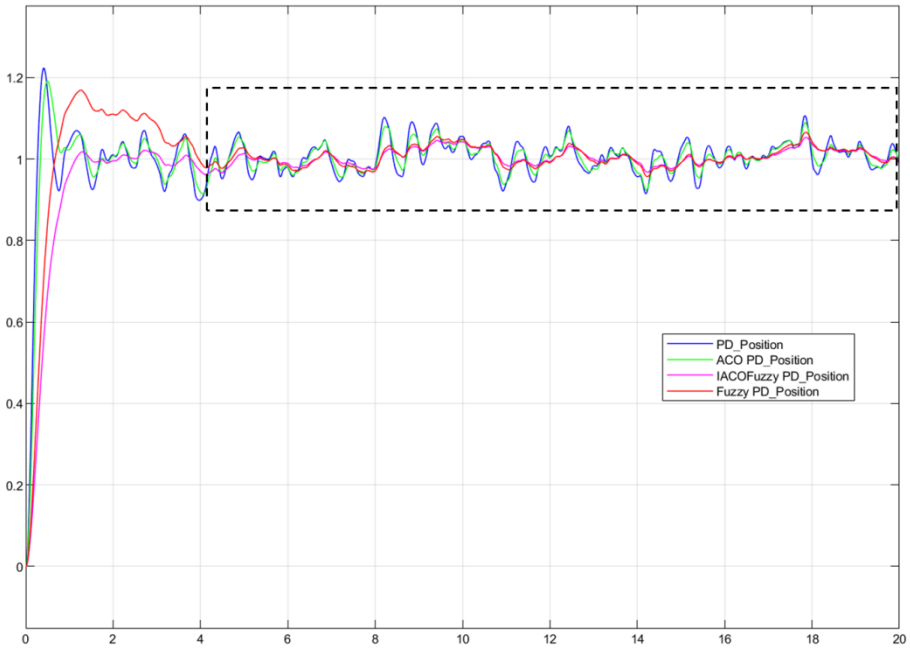

Fig. 12. Position response curve under disturbance signal (Photo credited: Original)

Table 4. Position control performance comparison under disturbance signal

	Max Value	Min Value	Difference
PD	1.106	0.9055	0.201
ACO PD	1.089	0.9143	0.1751
Fuzzy PD	1.066	0.9568	0.109
IACO Fuzzy PD	1.053	9.617	0.09154

From Fig. 12. can be seen that the IACO Fuzzy PD has the smallest interval of oscillation under perturbation and the most stable signal with strong robustness. As shown in the Table 4, the oscillation range of IACO fuzzy PD is only 0.09154.

5.4 Signal Following

The follow signal has a mean of 5, a variance of 1, and a sampling time of 3s. From Figure 13, it can be seen that IACO Fuzzy PD responds quickly, with good stability and without overshoot.

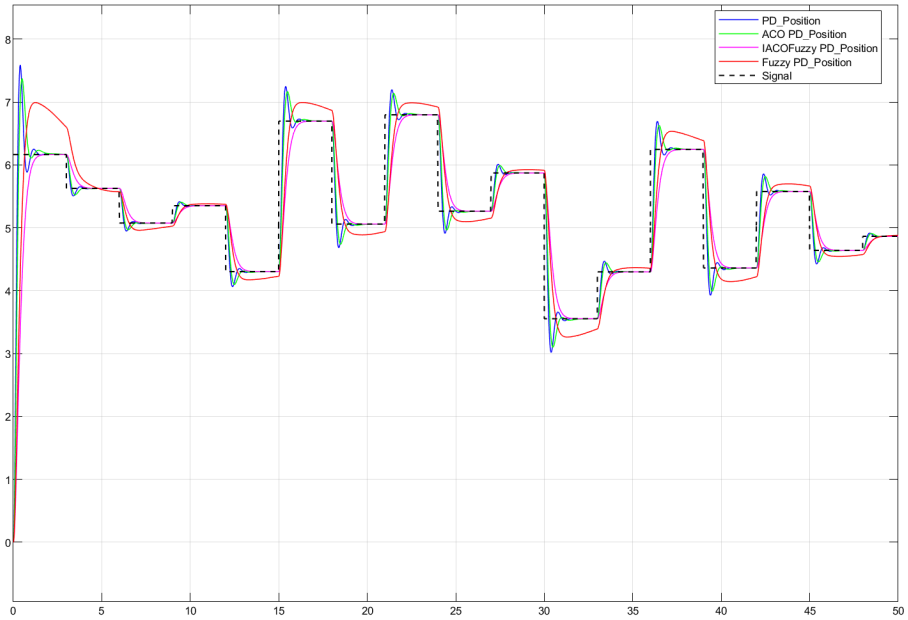

Fig. 13. Position response curve with following signal (Photo credited: Original)

6 Conclusion

In this paper, a fuzzy PD controller is optimized based on the improved ant colony optimization to improve the speed and accuracy of the position control of BLDC. The BLDC mathematical model is developed, and a fuzzy PD controller based on the improved ant colony optimization is designed by optimizing the parameters of the fuzzy PD using IACO. The closed-loop position control simulation model of BLDC is constructed by Simulink platform of MATLAB, and the PD, fuzzy PD, ACO PD and IACO fuzzy PD are compared. The simulation results demonstrate that there is no overshoot amount and that the required IACO response time under the unit step signal is 1.756 s; under the perturbation signal, the peak-to-peak difference of IACO is only 0.09154; under the tracking signals of different positions, the performance of IACO is still excellent with good tracking ability and stability. Therefore, following a comparison of the four algorithms' simulation results, it is concluded that IACO can effectively shorten the response time and the system overshoot amount, improve the dynamic performance and stability of the system, and has robustness.

Reference

1. Wang W. Research on intelligent optimization of fuzzy control for brushless dc motor[D]. Guilin University of Technology, 2022.

2. Huynh V. N. and Dang X. B. An adaptive PID controller for precisely angular DC motor control, JTE, 17(1), 48–55 (2022).
3. Liang Hongji, Li Junli, Zhang Yuanyao: Trajectory tracking control of four-rotor UAV based on auto-coupled PD [J]. Journal of Shaanxi University of Technology (Natural Science Edition), 40(01): 47-55+79 (2024).
4. Xing W. Guo X. Xiao J. Research on Sliding Mode PD Control of Lower Limb Exoskeleton Walking Aid Robot.Chinese Journal of Biomedical Engineering, 41(05):621-625 (2022).
5. Tsai C. -C. Chan C-K, Shih S-C. and Lin S. -C. Adaptive nonlinear control using RBFNN for an electric unicycle, 2008 IEEE International Conference on Systems, Man and Cybernetics, Singapore, 2343-2348 (2008),
6. Zhao H. Research on Drive Control of Intelligent Mower [D].Zhejiang University,2020.
7. Zhao K, Zeng T. Fuzzy PID control of phase-shifted full-bridge based on improved particle swarm optimization [J]. Journal of Xiamen University(Natural Science), 63(02):259-270 (2024).
8. Xu J. Chen F. Position Control of Hybrid Stepper Motor on BSO Improved Fuzzy Neural Network PID Algorithm [J/OL]. Mechanical Science and Technology for Aerospace Engineering: 1-10 (2024).
9. Fang W. AI Shi-zhong, WANG Qing, FAN Jun-bo: Research on Cold Chain Logistics Distribution Path Optimization Based on Hybrid Ant Colony Algorithm[J].Chinese Journal Of Management Science, 27(11):107-115 (2019).
10. Li Z. Position Sensorless Control for BLDCM Based on Modified Neural Network [D].Harbin Institute of Technology, 2021.
11. Shi L. Research on Brushless DC Motor Servo Control System Based on PID Algorithm[D].Northeastern University ,2022.
12. Wei X. Numerical study of tuning parameters of indoor temperature PID controller and supply air volume PI controller based on improved ant colony algorithm for an air-conditioning fan coil unit and its control performance [D]. Lanzhou University of Technology, 2019.